

Dynamics of directional selectivity in MT receptive field centre and surround

János A. Perge, Bart G. Borghuis, Roger J. E. Bours, Martin J. M. Lankheet and Richard J. A. van Wezel

Functional Neurobiology, Helmholtz Institute, Faculty Biology, Utrecht University, Padualaan 8, 3584 CH, Utrecht, the Netherlands

Keywords: electrophysiology, extrastriate cortex, macaque monkey, middle temporal area, motion perception

Abstract

We studied receptive field organization of motion-sensitive neurons in macaque middle temporal cortical area (MT), by mapping direction selectivity in space and in time. Stimuli consisted of pseudorandom sequences of single motion steps presented simultaneously at many different receptive field locations. Spatio-temporal receptive field profiles were constructed by cross-correlating stimuli and spikes. The resulting spike-triggered averages revealed centre-surround organization. The temporal dynamics of the receptive fields were generally biphasic with increased probability for the preferred direction at short latency (50–70 ms) and decreased probability at longer latency (80–100 ms). The response latency of the receptive field surround was on average 16 ms longer than that of the centre. Our results show that surround input and biphasic behaviour reflect two different mechanisms, which make MT cells specifically sensitive to motion contrast in space and time.

Introduction

Motion detection is altered when a moving pattern is surrounded by other patterns moving either in the opposite or the same direction (Murakami & Shimojo, 1996; Tadin *et al.*, 2003; Betts *et al.*, 2005). These surround influences on perceptual motion sensitivity are generally supposed to reflect spatio-temporal tuning properties of visual motion-sensitive neurons.

Numerous studies have established a close link between neural activity of neurons in the middle temporal cortical area (area MT or V5) in primates and motion perception (Britten *et al.*, 1992; Britten & Newsome, 1998). Neurons in MT respond selectively to a particular subset of directions and speeds of motion within their receptive field (Dubner & Zeki, 1971; Maunsell & Van Essen, 1983; Albright, 1984; Mikami *et al.*, 1986). For about 50% of MT neurons the response to the preferred direction in the receptive field centre is suppressed by the same direction in the surrounding area (Allman *et al.*, 1985; Born & Tootell, 1992; Raiguel *et al.*, 1995; Xiao *et al.*, 1995; Born, 2000). This phenomenon, often referred to as centre-surround antagonism, makes neurons specifically sensitive to motion contrast, and thus supports a role in relative motion perception. Because physiological properties of MT neurons reflect the requirements for relative motion perception, characterizing the spatial and temporal properties of centre-surround interactions may reveal its neural basis.

Spatio-temporal receptive fields can be reconstructed by flashing bright and/or dark stimuli pseudorandomly at different spatial locations and cross-correlating the neuronal spike train to the stimulus sequence. This luminance reverse correlation method has been used extensively to describe receptive fields of neurons in the retina (Rowe & Palmer, 1995), the lateral geniculate nucleus (LGN; Reid *et al.*, 1991, 1997; Cai *et al.*, 1997) and primary visual cortex (V1; Reid *et al.*, 1991; DeAngelis *et al.*, 1995; Ringach *et al.*, 1997, 2003; De

Valois *et al.*, 2000; Dragoi *et al.*, 2002; Mazer *et al.*, 2002). For neurons that behave approximately linearly, such as those in LGN or simple cells in V1, first-order correlation between stimulus and response provides a fairly complete description of spatio-temporal receptive field properties. However, for motion-sensitive neurons first-order correlation fails to capture the essential tuning properties like motion direction and speed selectivity. Therefore, second-order analysis (i.e. the combination of two stimuli presented at different locations and different times) is required to reconstruct the relevant receptive field characteristics.

Second-order analysis of dark and/or bright stimuli has been used to characterize direction selectivity in cat simple and complex cells (Emerson *et al.*, 1992), as well as in motion-sensitive macaque area MT (Livingstone *et al.*, 2001; Cook & Maunsell, 2004). One disadvantage in studying motion sensitivity using these luminance reverse correlation techniques is that the motion energy for specific motion directions is very small compared with the motion energy of coherently moving patterns. Luminance-based reverse correlation is therefore limited in revealing complex spatio-temporal receptive field properties of motion-sensitive cells. To overcome this problem, Borghuis *et al.* (2003) proposed a motion reverse correlation method, which employs a pseudorandom sequence of motion impulses. This motion reverse correlation method is much more effective in eliciting spikes, which allows for a detailed analysis of spatio-temporal receptive field properties of motion-sensitive cells.

In this study, we used a spatio-temporal version of the motion reverse correlation paradigm (Borghuis *et al.*, 2003) to investigate the dynamics of directional selectivity in MT receptive field centres and surrounds. We focus on two properties that are important for shaping directional responses in area MT: biphasic behaviour and centre-surround organization. We have previously shown that many MT cells display biphasic reverse correlation functions, indicating reduced sensitivity after a single step to the preferred direction (Perge *et al.*, 2005). Thus, biphasic behaviour makes MT neurons specifically sensitive to temporal motion contrast. Centre-surround organization,

Correspondence: Dr R. van Wezel, as above.

E-mail: r.j.a.vanwezel@bio.uu.nl

Received 12 February 2005, revised 21 July 2005, accepted 8 August 2005

on the other hand, makes MT cells sensitive to spatial motion contrast. Thus, MT neurons are sensitive to both spatial and temporal motion contrast. However, it is unclear whether these characteristics reflect a single mechanism or multiple mechanisms. In this study, we describe the dynamics of centre and surround responses, and show that biphasic response characteristics in the centre operate at a time scale distinctly different from delayed surround inhibition.

Materials and methods

Two adult male rhesus macaques (*Macaca mulatta*) participated in this study. Before the experiments, each monkey was implanted surgically with a head-holding device, a search coil for measuring eye movements using the double induction technique (Reulen & Bakker, 1982; Malpeli, 1998), and a stainless-steel recording cylinder placed over a craniotomy above the left occipital lobe. The surgical procedures were performed under N₂O/O₂ anaesthesia supplemented with isoflurane. After recovery, the monkeys were trained to fixate a rectangular spot ($0.4 \times 0.4^\circ$) on a black background. During the experiments, each monkey sat in a primate chair 57 cm from a cathode ray tube display. Eye movement recordings were sampled at 500 Hz. For accurate fixation, the monkeys had to maintain their viewing direction within a virtual fixation window around the fixation point (2° in diameter). While correctly fixating, the monkey was rewarded with water or juice every 3 s. The average fixation period was 4.4 s. Breaking fixation resulted in pausing the presentation of stimuli and no reward. Stimulus presentations were restarted after 300 ms of correct fixation. Animal procedures used in this study were approved by the Animal Use Committee (DEC) of Utrecht University, and procedures followed national and international guidelines.

Neuronal recordings

Single-unit recordings were carried out using standard extracellular methods. During experimental sessions, a parylene-insulated tungsten microelectrode ($0.5\text{--}2\text{ M}\Omega$ at 1 kHz) was inserted manually through a guide tube and then manipulated by a micropositioning controller. Area MT was identified by the recording position and depth, the transition between grey matter, white matter and sulci along the electrode track, and by its functional properties. Among others, these are the prevalence of direction-selective units, the similarity in direction tuning for nearby single-unit recordings, the receptive field size according to eccentricity and the change of direction tuning along the electrode penetration. We have no histological confirmation of the recording sites because both monkeys are currently being used in other experiments. Spike times were registered at 0.5 ms resolution for on-line analysis and data storage, using a Macintosh G4 computer with a National Instruments PCI 1200 data acquisition board.

Stimuli and experimental procedure

The monitor (Sony Trinitron Multiscan 500 PS) was driven by an ATI Rage graphics card. The refresh rate was 75 Hz (1152×870 pixels) for early experiments in monkey A (10 cells recorded in monkey A), and 120 Hz (1024×768 pixels) in all other experiments. The stimulus was a rectangular field presented on a black background and it was divided into smaller subfields along an invisible grid (Fig. 1). Each subfield contained a high-density binary random dot pattern, consisting of 50% black and 50% white dots (Julesz, 1971). Mean luminance of the stimulus was 48 cd/m^2 . A dot size of

$0.14 \times 0.14^\circ$ was used for 10 cells in monkey A, and $0.20 \times 0.20^\circ$ for all of the remaining cells.

The stimulus was positioned over the receptive field centre as determined by hand mapping. In each subfield pattern the dot pattern was shifted each monitor frame (8.3 ms at 120 Hz and 13.3 ms at 75 Hz) or every second monitor frame (17 ms at 120 Hz and 27 ms at 75 Hz). The size of the shift was 0.14° in horizontal and vertical directions, and 0.15° in diagonal directions. As determined by the motion reverse correlation method, the shifts occurred in either the preferred or the anti-preferred direction (Borghuis *et al.*, 2003; Perge *et al.*, 2005) and in a pseudorandom order (Fig. 1A and B). The anti-preferred direction was defined as the direction opposite to the preferred direction. The dot displays in the subfields were presented simultaneously, and the direction in a subfield chosen at each motion step was independent from the directions in other subfields. Between different experiments, the number of subfields varied. The resulting sequence of motion steps effectively stimulated most of our neurons. In case the stimulus did not drive the neuron effectively, the size of the shift was either increased or decreased in a range of $0.07\text{--}0.42^\circ$ (in steps of 0.07°) until a sufficiently strong response was obtained. The motion steps in the preferred and anti-preferred direction in each subfield were presented 7000–8000 times in a randomized order. This number was increased if the signal-to-noise ratio of the online analysis was judged insufficient. A movie demonstration of the stimulus is available at our website (see Supplementary material section) Stimulus generation, data collection and monitoring the monkeys' performance was done by custom-made software written in programming language C. Offline data analysis was done in MATLAB.

Stimulus size and the number of subfields were optimized for each cell. We tried to maximize spatial resolution of the measurement by increasing the number of subfields while decreasing their size. However, by decreasing the size of the subfields the effective stimulus energy also decreases substantially. As a result, responses as well as the signal-to-noise ratio in the measurement decrease. Therefore, we needed a balance between sufficient spatial resolution and excitability. We found that subfields of minimally $1.5 \times 1.5^\circ$ stimulated most recorded neurons properly. For cells with insufficient responses, we increased the size of the patches until an adequate response was obtained.

Data analysis

We used the method of spike-triggered averaging (de Boer & Kuyper, 1968) to estimate the properties of spatio-temporal receptive fields in area MT (Fig. 1B and C). We calculated the average stimulus preceding the spikes as a function of time, t . The stimulus was represented by a temporal sequence of motion impulses for each stimulus patch, where +1 and -1 indicate the occurrence of preferred and anti-preferred directions, respectively. Spike-triggered averages (STAs) for each location were obtained by calculating the average stimulus value preceding each spike at that location. Thus, the resulting STA fluctuates in time between +1 and -1, where positive values indicate a relatively higher probability for the preferred motion direction and negative values indicate a relatively higher probability for the anti-preferred motion direction to occur at time t before the spikes. A value of zero indicates that preferred and anti-preferred stimulus direction occurred with equal probability at that time. STAs were smoothed by sliding window averaging with a Gaussian profile (standard deviation of 8 ms), which removed most of the noise without affecting the overall shape of the function and its main parameters (Perge *et al.*, 2005).

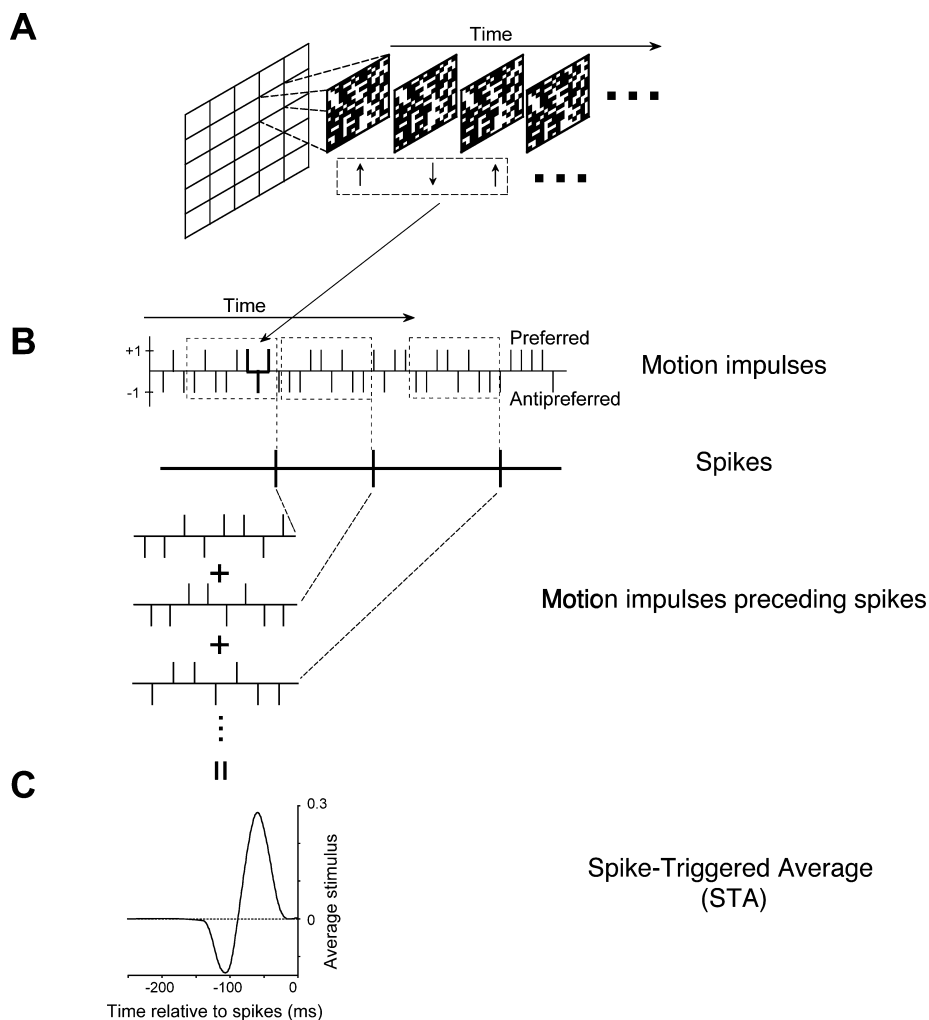


FIG. 1. Illustration of the stimulus and the motion reverse correlation paradigm. (A) Stimuli were random dot patterns (50% dark and 50% white dots) presented simultaneously at different locations along a grid of squares. Each dot pattern within a subfield of the grid was shifted either to the preferred or anti-preferred direction of the neuron in a pseudorandom order. (B) Representation of the stimulus sequence and the reverse correlation procedure. The values of +1 and -1 indicate motion impulses to the preferred or anti-preferred direction, respectively, for one subfield. (C) Equal length stimulus sequences preceding the spikes were collected and averaged. This results in a spike-triggered average (STA) for each individual subfield.

A significance criterion for the STAs was determined by calculating the mean and standard deviation of the STA based on a period of 100 ms following spikes in all subfields. This section of the STA reflects the noise in the STAs as it indicates random correlations between spikes and stimuli presented after the occurrence of the spikes. We used an arbitrary noise level of four standard deviations for defining significant excursions in the STA.

Results

Spatio-temporal receptive fields were mapped with the spatial reverse correlation technique (see Materials and methods) in area MT of two male rhesus macaque monkeys for a total of 56 neurons (40 neurons in monkey A and 16 in monkey S). Figure 2 shows the results for one example cell. This neuron was tested at 64 locations along an 8×8 grid of subfields with random dot patterns moving simultaneously either in the cell's preferred or anti-preferred direction. Responses were reverse-correlated to the stimulus sequence for each subfield of the stimulus (see Materials and methods, and Fig. 1), resulting in individual STAs for each individual stimulus subfield (Fig. 2A). The two subfields with high values (high probability for the preferred

direction) correspond to the centre of the receptive field. The subfields with low values correspond to the surround. Because the STAs show the average stimulus in time, Fig. 2A reveals both the temporal dynamics and the spatial characteristics of the receptive field.

The difference in the time course of the STAs is more salient when the STAs are presented on top of each other (Fig. 2B). Two representative STAs were plotted with thicker lines. One STA with the large amplitude corresponds to a subfield covering the centre of the receptive field and another one with small negative amplitude corresponds to a subfield covering the surround. The STA corresponding to the centre shows strong correlation with the preferred direction peaking at about 60 ms prior to the spikes. At longer delays, however, the STA changes in sign showing a dip at about 110 ms prior to the spikes indicating a stronger correlation with the anti-preferred direction. This biphasic characteristic indicates that spike generation is suppressed after the initial response to the preferred motion impulse. For this example MT neuron the time course of STAs in the surround is delayed by 10 ms relative to that for the centre. This difference in latency does not correspond to the delayed suppression in the centre, which is at about 110 ms. Thus, Fig. 2B shows that for this cell, temporal dynamics for centre and surround are clearly different.

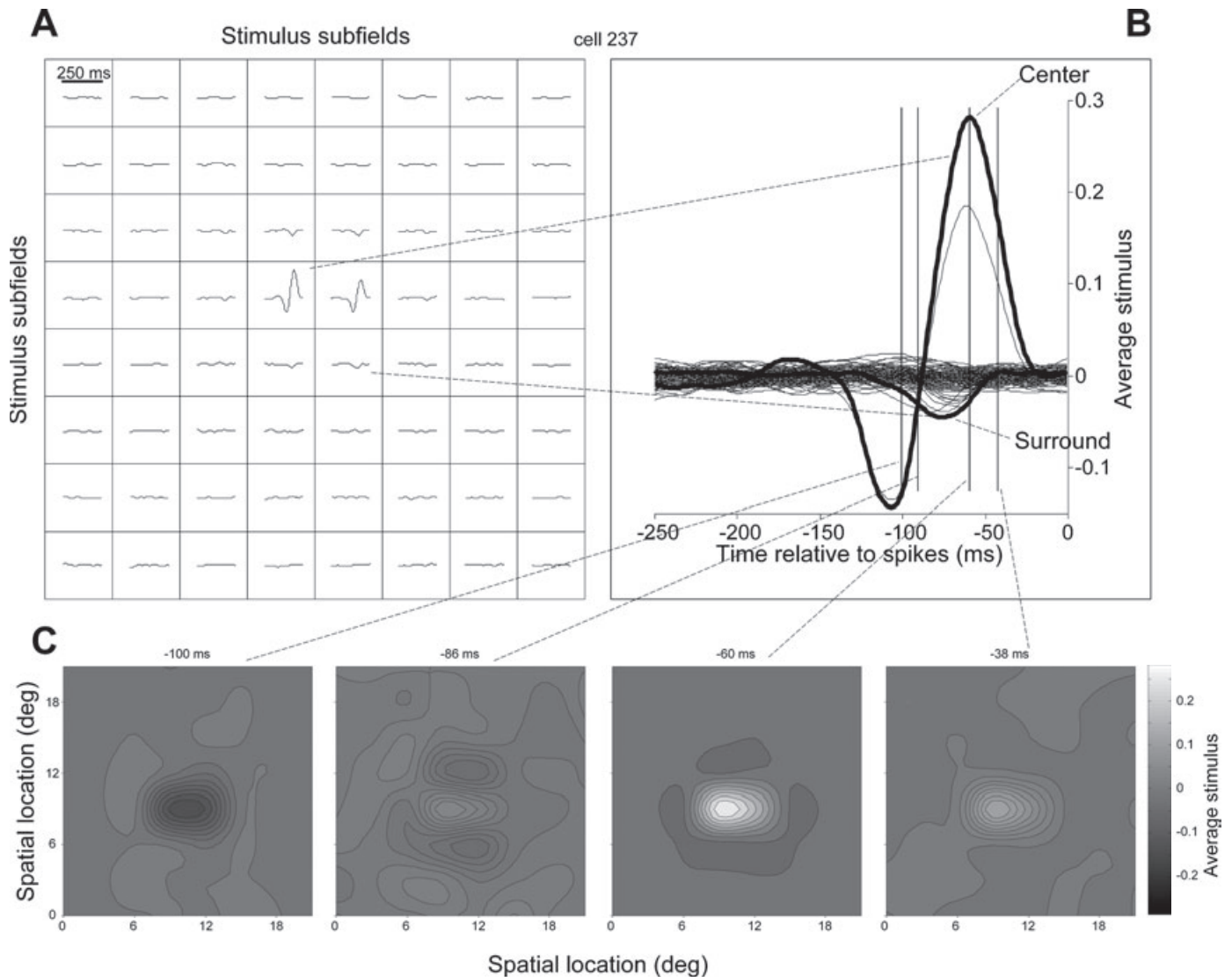


FIG. 2. Spatio-temporal receptive field of one example MT neuron. (A) The stimulus consisted of an 8×8 grid of stimulus subfields moving independently in either the preferred or anti-preferred direction. At each stimulus subfield, the STA for that location is plotted. The rightward point of each individual curve indicates the average stimulus value at 0 ms before the occurrence of a spike (by definition this will always have an average stimulus value of 0). The leftward point of the curve is the average stimulus value 250 ms before a spike occurred. (B) The same STAs as in (A) plotted on top of each other. The two thick lines with the large and small amplitude indicate STAs for a centre and a surround subfield, respectively. (C) Spatial receptive field representations shown at four different times before the spikes occurred as indicated by the vertical lines in (B). The contour plots were derived by linear interpolation between average stimulus values at adjacent positions in the 8×8 grid. White shading indicates high average stimulus values (higher probability for a preferred direction). Dark shading indicates a low negative average stimulus value (higher probability for an anti-preferred direction). The x and y coordinates indicate the distance from the bottom left of the stimulus field in visual degrees. The distance from the fixation point to the centre of the stimulus field was 11.1° .

A spatial representation of the receptive field can be constructed at each delay of the STAs. These spatial receptive field maps were derived by linear interpolation between probability values of the STAs at adjacent spatial locations. Such receptive field maps are shown for four different delays preceding the spikes (Fig. 2C). The total series of spatial receptive field maps at each delay is shown in a movie (see Supplementary material section). These maps reveal the spatial organization of a centre-surround receptive field structure in time, revealing the different temporal dynamics of centre and surround responses. The results in Fig. 2 show that the cell responses are modulated by the surround, but whether this is due to excitation for anti-preferred directions or inhibition for preferred directions in the surround can not be determined from our analysis. The analysis does not imply that the cell would be excited when the surround alone

would be stimulated in the null direction. The results show that the surround modulates the response, while stimuli are presented throughout the receptive field simultaneously.

In general, surround responses were relatively weak. Sometimes the surround was radially symmetric (as the example cell in Fig. 2), but very often it was irregular and patchy. The irregularities partly could arise due to the limited spatial sampling resolution of our stimulus, as we only used a limited number of subfields (grids of 5×5 to maximum 10×10 subfields). However, for some recordings the irregularities are clearly due to intrinsic inhomogeneities of the receptive field, as has been reported by others (Raiguel *et al.*, 1995).

In Fig. 3, we show five example cells that are representative for our whole population. Because the two spatial and one temporal dimension are difficult to visualize in a single plot we present the

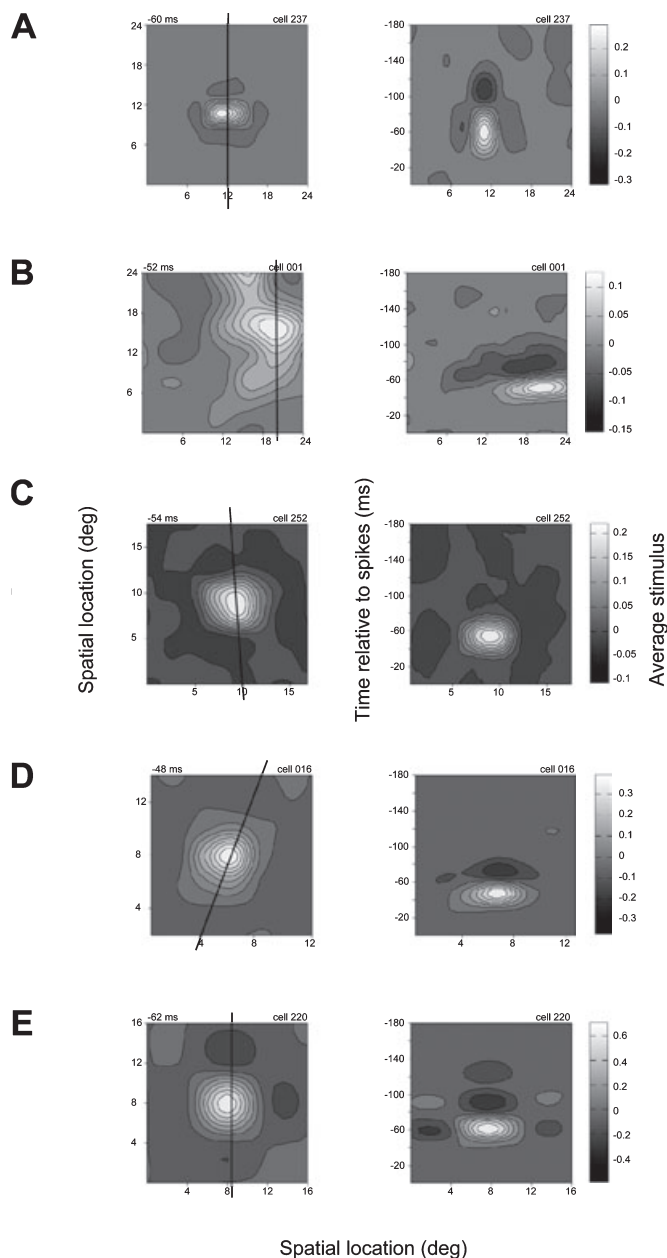


FIG. 3. Spatio-temporal receptive field maps of five example MT neurons. Left column: spatial receptive field profile at the time where the STA reaches its maximum (maximal correlation between stimulus and response). This time of maximal correlation is indicated at the upper left part of each subfigure. Figure 3A is the same cell as plotted in Fig. 2. The x and y coordinates indicate the distance from the bottom left of the stimulus field in visual degrees. The distance from the fixation point to the centre of the stimulus field for cells A–E was 11.1, 11.8, 3.9, 6.7 and 5.9°, respectively. Oriented bars indicate a representative cross-section of the receptive field, containing both centre and surround regions. Right column: a representative cross-section of the spatial receptive field maps plotted as a function of time relative to the spike occurrence reveals the temporal development of the receptive field.

spatial and temporal characteristics separately. The left-hand column of Fig. 3 shows the spatial receptive field maps at the correlation delay where STAs reach their maximum value, similar to the -60 ms plot of Fig. 2C. Note that a surround is not necessarily visible in these subfigures, because the surround generally has a longer latency.

To show the temporal characteristics of the receptive field for the same neuron, we plotted an informative cross-section of the receptive field at different times relative to the spike occurrence (right-hand column). This cross-section is indicated by orientated bars in the left-hand column and contains both the maximum value for the centre and the minimum value for the surround at any delay. The centre was defined as the subfield with the highest STA value, and the surround was the subfield with the lowest STA value (high correlation with the anti-preferred direction) during the short latency phase. The right column in Fig. 3 shows the resulting plots for the five example cells, and illustrates the diversity in receptive field characteristics that we observed.

For some cells, the latency for the surround was close to that of the negative phase for the centre. For these cells, the surround and the long latency negative phase of the centre were intermingled (Fig. 3A, the same neuron as presented in Fig. 2). Figure 3B is an extreme example of such a cell with a biphasic response and surround that are indistinguishable. Figure 3C shows a neuron without a long latency negative phase, which we will label a monophasic response. Some of the other cells, such as the example cell in Fig. 3D, showed no clear surround. For the last example cell (Fig. 3E), both centre and surround show biphasic temporal characteristics. The short latency phase of the surround and the long latency phase of the centre are clearly separated in time for this cell. The example cells in Fig. 3 suggest that spatially separable surrounds and biphasic temporal profiles result from different mechanisms. The following section addresses the temporal dynamics of these two features quantitatively.

To estimate the size of the receptive fields, we used the spatial receptive field maps at the correlation delay where STAs reach their maximum value. We fitted these maps with a two-dimensional radially symmetric Gaussian. We only used those receptive field maps that showed at least three subfields with significantly high STA values (four standard deviations above noise level, see Materials and methods). In our recorded population, 41 cells (73%) fulfilled this criterion. The receptive field diameter was defined as the width of the Gaussian fit at half height.

The average receptive field diameter in our population was $10.7 \pm 4.8^\circ$ at an average eccentricity of $10.9 \pm 5.0^\circ$. This is in agreement with previous reports (e.g. Rodman & Albright, 1989; Raiguel *et al.*, 1995). We applied a linear regression to investigate the relationship between the area of the receptive field and eccentricity similar to the method described by Raiguel *et al.* (1995). The log-linear regression of the receptive field surface and eccentricity had a slope of 0.02 ($r^2 = 0.04$), which is similar to previous studies reporting receptive field sizes in MT using similar stimuli and data-analysis (Raiguel *et al.*, 1995).

Differences in centre and surround dynamics

To quantify the temporal differences between centre and surround for our population of cells, we analysed the time course of the STAs at different locations in the receptive field. The centre of the receptive field was defined by subfields that showed a significant increase in average value. A stimulus subfield was defined as a surround subfield if the STA at that location did not show a significant increase but only a decrease in average stimulus value. Our significance criterion was four standard deviations (see Materials and methods) above or below zero. Using this surround definition, 28/56 neurons (50%) showed the presence of a surround.

In most recordings (75% of the cells with a surround) more than one stimulus subfield showed the presence of an antagonistic surround.

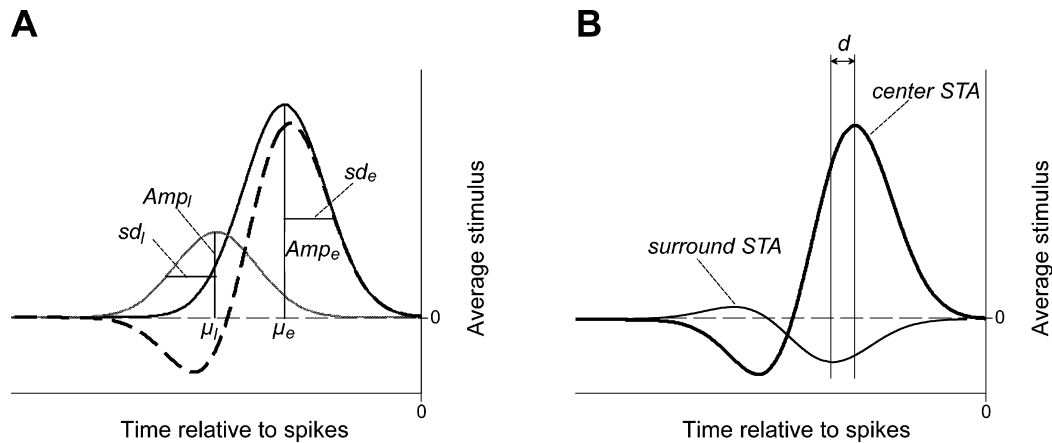


FIG. 4. Illustration of our model describing the temporal dynamics of the spatial receptive field. (A) The temporal profile of our model consists of an early (thin black line) and late (thick line) Gaussian profile. The difference between the early and late components results in a biphasic profile (dashed black line). Amp , amplitude; sd , height at half width; μ , time of the peak. Subscripts e and l refer to the early and late components, respectively. (B) The centre and surround temporal profiles are both separately constructed according to Fig. 4A. For more details, see the description in the text. d , difference in time between the temporal profiles of the centre and surround.

Peak latencies for the corresponding STAs were not significantly different. This observation was also confirmed by a more quantitative analysis of the shape of the STAs (see next paragraphs). For this reason we averaged all surround STAs and we used this average surround STA in later analysis.

Figure 4A illustrates the model that we used to quantify the temporal changes of centre and surround. The model consisted of two Gaussian functions, one for the early (thin black line) and one for the late component (grey line). The time course of the centre STA was then described as the difference of these two Gaussians according to the form:

$$DOG_{cen}(t) = A_e \times \frac{1}{\sqrt{2\pi} \times sd_e} \times e^{-\frac{1}{2} \left(\frac{t-\mu_e}{sd_e}\right)^2} - A_l \times \frac{1}{\sqrt{2\pi} \times sd_l} \times e^{-\frac{1}{2} \left(\frac{t-\mu_l}{sd_l}\right)^2} \quad (1)$$

where A_e and A_l are the surface area of the early and late components, μ_e and μ_l are the time of the peaks of the early and late components, and sd_e and sd_l represent the half-widths of the two Gaussians. The amplitude of the early and late components were obtained from equation 1 for $t = \mu$.

$$Amp_e = \frac{A_e}{\sqrt{2\pi} \times sd_e} \quad \text{and} \quad Amp_l = \frac{A_l}{\sqrt{2\pi} \times sd_l} \quad (2)$$

The DOG model accurately describes the different types of biphasic profile (the thick dashed line in Fig. 4A). The function describing the surround STA was similar to the function for the centre STA except that two additional free parameters (d and g) were introduced:

$$DOG_{sur}(t) = -g \times A_e \times \frac{1}{\sqrt{2\pi} \times sd_e} \times e^{-\frac{1}{2} \left(\frac{t-\mu_e+d}{sd_e}\right)^2} + g \times A_l \times \frac{1}{\sqrt{2\pi} \times sd_l} \times e^{-\frac{1}{2} \left(\frac{t-\mu_l+d}{sd_l}\right)^2} \quad (3)$$

where d is the delay between centre and surround, and g is a gain factor to scale the surround amplitude relative to the centre. The minus sign before g indicates that in our model the surround STA is

reversed with respect to the centre STA. In case more subfields fulfilled the criteria for surround, each surround STA was fit separately with different g and d parameters. The fits were carried out using a least-square minimization algorithm (Gauss–Newton method). The choice for our model was arbitrary, and it was chosen because it describes the data well. For example, a difference of gamma functions (Cai *et al.*, 1997) instead of Gaussian functions would provide similar results.

It is important to note that we assume similar shapes of the temporal profiles for centre and surround. Comparable models with the same assumption have been applied earlier to describe the temporal characteristics of visual receptive fields with delayed surround (Dawis *et al.*, 1984; Adelson & Bergen, 1985; Cai *et al.*, 1997). To evaluate the validity of this assumption, we calculated fit errors of surround STAs by subtracting our fit results from the original STAs. We found no systematic fit error over time, which supports our assumption of similarity in shape for centre and surround.

First, we analysed the differences in surround latencies at different spatial locations for the same neuron, for cells with multiple surround subfields under our definition. In general, we found that fit parameters indicating the surround delay relative to the centre delay (d) were similar within one measurement. For five neurons the number of surround fields was larger than three. For these cells, the average standard deviation of d was 5 ms, which was smaller than the variation in d within cells (see later). Because the surround fields showed similar temporal characteristics, we averaged all surround STAs within a measurement. Thus, the following results are based on fit results of the average surround STAs for each cell.

Figure 5 shows the delay of the centre early component (μ_e) plotted against the delay of surround early component ($\mu_e + d$). Most of the data points are above the diagonal, indicating longer surround latencies than centre latencies. The average delay difference between centre and surround was 16 ± 10 ms, which clearly differs from the delay difference of the early and late components both in the centre and surround ($\mu_l - \mu_e$, 39 ± 36 ms). We found no significant correlation between the difference of centre and surround delay and receptive field eccentricity ($r = -0.07$, $P > 0.05$), and found no significant correlation between the difference of centre and surround delay and the average distance of centre and surround field ($r = 0.01$, $P > 0.05$).

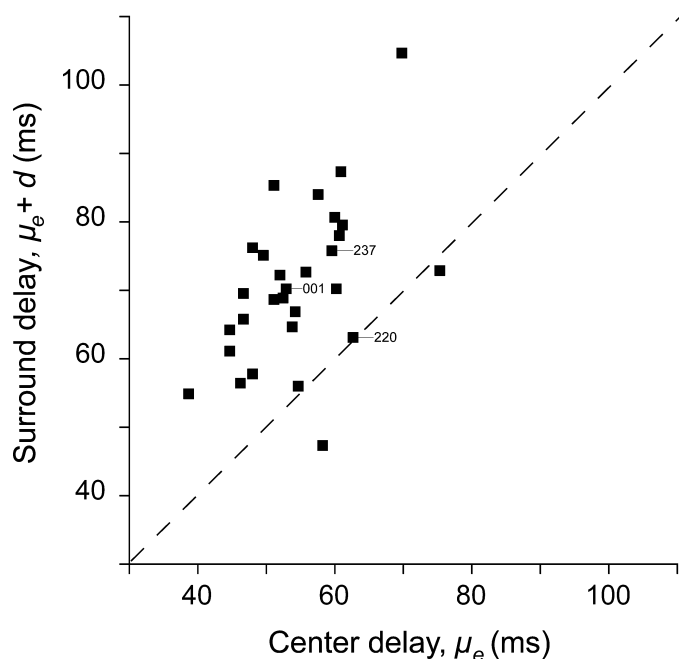


FIG. 5. Surround delay is longer than centre delay. Based on the model we describe in Fig. 4, we fitted the STAs for each cell separately, and plotted the centre delay (μ_{exc}) vs. surround delay ($\mu_{exc} + d$). Each symbol indicates one neuron. Only those neurons are shown where the minimum stimulus value of the surround was significant, i.e. more than four standard deviations below zero (50% of the neurons, $n = 56$). The average delay difference between centre and surround was 16 ± 10 ms. The dashed line indicates the line of equality. Numbers indicate the cell numbers of the cells shown in Fig. 3.

To characterize the magnitude of biphasic behaviour in the population, we computed a biphasic index (BI) for each neuron as the ratio of the amplitudes of the early and late components.

$$BI = Amp_1 / Amp_e \quad (4)$$

Thus, a low BI value corresponds to lack of biphasic behaviour and a high value to strong biphasic behaviour. Figure 6 shows the distribution of BI values across our population of recorded MT neurons. The mean BI for all of the cells was 0.40 ± 0.25 ($n = 56$). As Fig. 6 shows, a broad range of biphasicness was present in the population.

The black part of the bars in Fig. 6 indicates the number of neurons with a surround according to our significance criteria described earlier. The figure shows no clear relationship between the presence of surround and the strength of biphasic behaviour. To further investigate the relationship between biphasic behaviour and surround strength, we plotted the BI against g , a fit parameter indicating the strength of the surround relative to the centre (Fig. 7). We found no significant correlation between surround strength and biphasicness ($r = -0.04$, $P > 0.05$). This finding again indicates that biphasic behaviour and surround are not related to each other.

Second-order interactions

Antagonistic surrounds of MT cells described previously do not evoke excitation or inhibition themselves, but they modulate the responses to stimuli in the centre (Maunsell & van Essen, 1983; Allman *et al.*, 1985). The fact that we find surround effects in the STAs indicates that surround stimuli modulated the response irrespective of the centre

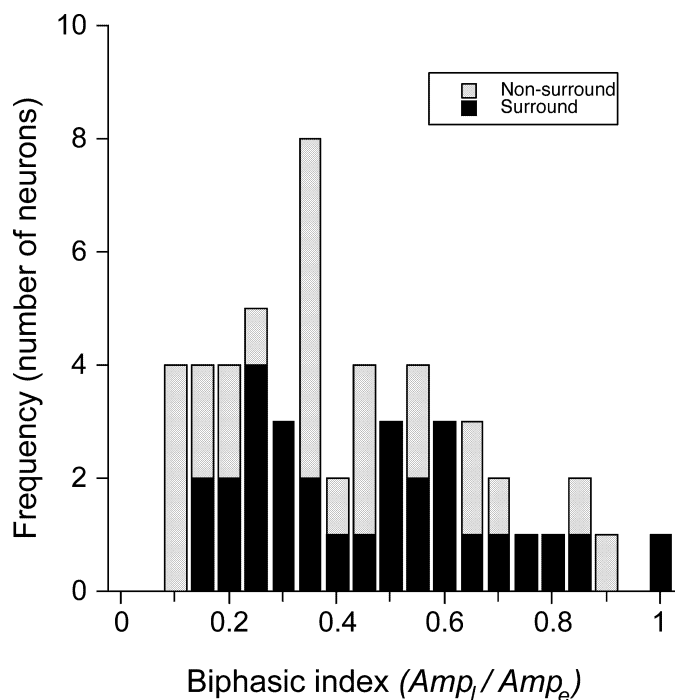


FIG. 6. The distribution of BIs indicating the biphasic temporal characteristics in the population ($n = 56$). A BI of 0 means complete lack of biphasic behaviour. Two outliers with a BI > 1 are not shown in this graph. The average BI was 0.40 ± 0.25 ($n = 56$). The black part of the bars indicates the number of neurons with surround using our significance criteria (see text).

stimulus. However, one cannot exclude the possibility that the modulation we observed was due to a specific combination of centre and surround stimuli. To clarify the role of specific directional interactions in generating surround modulations, we performed an additional second-order analysis.

We investigated how specific combinations of centre and surround subfields modulate responses and how much they deviate from a linear prediction, which assumes independence of responses. The general idea of this analysis is similar to that described in detail in our previous paper on interactions between different motion directions (Perge *et al.*, 2005). In short, we calculated second-order reverse correlograms, i.e. correlation functions for stimulus pairs in centre and surround subfields. We compared these correlograms to predicted second-order correlograms, which were calculated based on the assumption that subfields interact only in a linear manner (summation). To obtain predicted second-order correlograms we multiplied the first-order correlograms of the individual subfields (preferred direction in centre and surround).

In the presence of specific non-linear interactions between centre and surround subfields, predicted and measured second-order correlograms differ. We expressed the deviations by subtracting the predicted second-order correlograms from the measured ones (prediction error). Thus, a zero value in the prediction errors indicates that summation properties can be approximated by linear summation. Significant positive or negative deviations suggest direction-specific interactions. We calculated prediction errors for all possible centre and surround combinations for all of the neurons showing the presence of a surround (28 neurons). Prediction errors for surround/centre, surround/surround and centre/centre combinations were averaged separately.

We expressed the level of non-linearity for surround/centre, centre/centre and surround/surround combinations by finding the

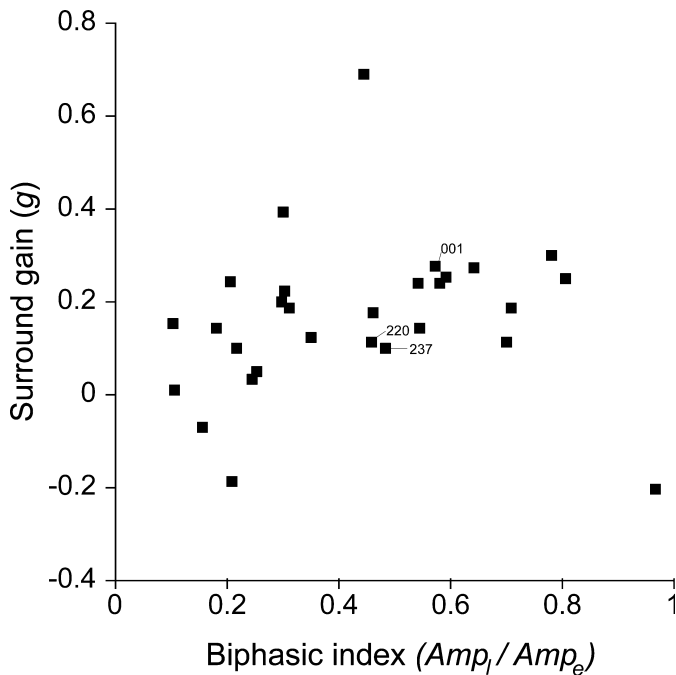


FIG. 7. Strength of biphasic behaviour and strength of surround are not correlated. Strength of surround was defined by fit parameter g (see text), which indicates the surround amplitude relative to the centre amplitude. Each symbol indicates one neuron. The r^2 -value of the linear fit was 0.0016 ($P > 0.05$). Numbers indicate the cell numbers of the cells shown in Fig. 3.

largest (positive or negative) value for the three conditions (average surround/centre, surround/surround and centre/centre prediction errors) within a predefined time window. This time window was acquired from the analysis of the centre STA with the largest amplitude, and corresponded to the duration where the STA was higher than four standard deviations (see Materials and methods). Different measurements had different noise levels in the prediction errors, which would make it difficult to compare individual recordings. Therefore, we normalized prediction errors to the standard deviation, which was calculated from the noise level of the uncorrelated part of the prediction errors (after spike occurrence).

Figure 8 shows the distribution of maximum prediction errors for surround/centre and centre/centre stimulus combinations in the population. The deviations from a 'linear' prediction for surround/centre stimulation showed a minor positive shift from zero (0.06 ± 1.25 , Fig. 8A). This shift was not statistically different from zero (t -test, $P = 0.79$). We found similar results for the surround/surround combination (mean = 0.52 ± 1.4 , t -test, $P = 0.18$, data not shown). These results indicate that, with our stimulus presentation and data analysis, the response modulation due to surround stimuli does not critically depend on a specific combination of centre and surround stimuli.

The only 'non-linear' interaction that we found was between centre subfields (mean = -2.38 ± 4.07 , t -test, $P = 0.005$, Fig. 8B). For six neurons (21% of the surround cells) the deviation from zero prediction error was larger than four standard deviations. The large negative prediction errors show that multiple centre stimuli are less effective than the sum of the mean individual effects, which might be due to response saturation. This result indicates that our analysis is able to detect expected non-linear interactions between stimulus subfields.

The above analysis targeted the non-linear effects of simultaneous stimulus pairs. Considering that centre and surround have different

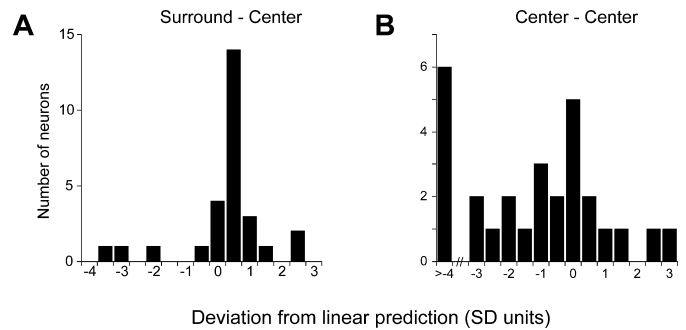


FIG. 8. Centre and surround second-order interactions. (A) Distribution of maximal prediction errors for surround-centre combination is statistically indifferent from zero, i.e. perfect linear approximation (t -test, $P = 0.79$). (B) Many cells show smaller responses than predicted for centre-centre combination, causing the distribution and its mean significantly different from zero (t -test, $P = 0.005$). Positive values on the abscissa correspond to larger while negative values correspond to smaller responses than expected from linear prediction. SD corresponds to the standard deviation of all prediction errors within a measurement.

response latencies, we also extended our analysis to stimulus combinations that were presented at different times. In this analysis the temporal separation between stimuli was one motion step, 26 ms in most experiments. We analysed the effect of subsequent stimulation of surround/centre, centre/surround, surround/surround and centre/centre subfields. None of these conditions showed a significant shift from zero prediction error when analysed at the population level (t -test, $P > 0.05$, data not shown).

Discussion

We have shown two important aspects of the temporal dynamics of area MT receptive fields. First, peak latency for the surround was on average 16 ms longer than that for the centre. Second, biphasic behaviour for full-field stimuli (Perge *et al.*, 2005) is also found for local responses in centre and surround. Even though the delayed surround response and the biphasic characteristics of the centre cannot always be separated in space and time, our results indicate that biphasic behaviour does not primarily result from centre-surround antagonism.

The antagonistic surrounds we report here are small compared with literature. Previous authors found a surround size up to 10 times the size of the centre (Allman *et al.*, 1985; Tanaka *et al.*, 1986), while others reported a factor of three–four (Raiguel *et al.*, 1995). Because our neurons appeared to show weak and spatially asymmetric surrounds, we did not attempt to characterize the size of the surround quantitatively. However, after the inspection of Fig. 3 it is evident that our surround sizes are even smaller than those reported by Raiguel *et al.* (1995). These differences might be related to different stimulus paradigms. We used binary noise stimuli, with rapidly changing motion directions, while previous reports were based on continuous stimulation of a much larger area of the surround. This may have resulted in lower estimates of surround size and strength in our data compared with previous reports.

We found no evidence for specific non-linear interactions between surround and centre. This result may seem surprising, as the antagonistic surround described in the literature is always considered to be a non-linear mechanism, because a stimulus presented in the surround alone does not evoke responses. However, what we show is that response modulation from surround stimuli does not depend on the simultaneous presence of an exciting centre stimulus. In all cases,

however, the effect occurred while stimuli were presented throughout the receptive field, causing sustained activity well above the spontaneous level. Our stimulus thus tends to 'linearize' responses and does not allow a clear distinction between non-linear suppression and 'linear' summation. The lack of a second-order effect seems to indicate that either the temporal resolution for non-linear interactions is too low to show up in our data, or the surround mechanism we describe is different from previously described non-linear surrounds.

The delay difference between centre and surround that we find is much shorter than the reported 40 ms in owl monkey MT (Allman *et al.*, 1985). This difference might again be due to differences in experimental paradigm. Allman *et al.* (1985) used continuous stimulation in the preferred direction, while we used a time-varying stimulus with two opposite motion directions. Temporal integration of motion responses for preferred and non-preferred directions thus may have affected the latency estimates in different ways.

It is interesting to note that area MT cells show receptive field properties in the motion domain similar to properties of low-level receptive fields in the luminance domain. However, delay differences between centre and surround responses are quantitatively different from findings at lower levels. Retinal P cells have a delay difference of 8 ms (Rowe & Palmer, 1995), and this value only increases slightly for LGN (10 ms, Cai *et al.*, 1997) and V1 (9 ms, Bair & Movshon, 2004). In contrast to the findings by Bair & Movshon (2004) for orientation tuning in V1, we found no evidence for a relationship between the strength of the surround and the difference in delay between centre and surround. Furthermore, we rarely observed the surround to be faster than the centre, which is described in V1 (Bair & Movshon, 2004).

Delayed surround effect might play a role in integrating local motion information into a global motion percept. For instance, it has been shown that area MT neurons first respond to local motion directions and gradually converge to a response to global motion directions (Pack *et al.*, 2001; but see Movshon *et al.*, 2003). Related to these reports are studies on pattern selectivity of MT neurons. Pattern direction selectivity is the ability to signal the single direction of a moving plaid instead of the two components of the plaid (Movshon *et al.*, 1985). Again, this ability develops in time during stimulation, though the time course of this effect is tens of milliseconds longer than our reported surround delay (Pack *et al.*, 2001; Smith *et al.*, 2005).

Several different models might explain delayed MT surround responses. A simple candidate would be localized spatial integration of V1 direction-selective responses to establish the centre, and more global integration of opposite directions with a reversed sign for the surround. This type of model was very successful in explaining monodirectional after-effects for bidirectional motion adaptation (Grunewald & Lankheet, 1996). It is not clear, however, where a delay difference of 16 ms would arise in such a model. Other options would be inhibitory input from MT neurons with a receptive field centre at the retinal location of the surround, tuned to the same direction (lateral inhibition) (Hartline *et al.*, 1956), or excitatory input from such neurons tuned to the opposite direction (disinhibition) (Allman *et al.*, 1985). Such lateral interactions require time, but again one would not necessarily expect such long delays. The longer latency that we observe could be related to the latency shifts of about 5 ms when inhibition is removed (Thiele *et al.*, 2004). Our results do not exclude the possibility that delay differences arise from feedback of higher visual areas (Bair & Movshon, 2004).

Our results show that MT neurons can have strong biphasic characteristics (Perge *et al.*, 2005). This characteristic could arise from short-term adaptation to a preferred stimulus. However, we showed in a previous paper that biphasic characteristics are not correlated with

the ratio between the transient and sustained response (Perge *et al.*, 2005), which characterizes short-term adaptation (Priebe *et al.*, 2002). Thus, biphasic responses reflect a different form of adaptation operating at a different time course. In this paper we also show that biphasic responses are not directly related to surround input. We found no correlation between biphasic behaviour and surround strength.

One might expect that the delay difference between centre and surround could also be observed at the level of motion perception. For V1 neurons, it has been shown that neural responses to temporally interleaved excitatory and inhibitory stimuli match perceptual masking (Macknik & Livingstone, 1998). Human psychophysical studies have shown that direction discrimination of random dots moving in a centre patch is strongly influenced by dots moving in the surround (Murakami & Shimojo, 1993, 1995, 1996). Depending on stimulus characteristics like centre size, eccentricity, etc. the centre dots can seem to move in the opposite direction (induced motion), or move in the same direction (motion capture). Our results suggest that the strength of motion capture and induced motion should be influenced by the timing of centre and surround onsets. Further psychophysical studies are required to confirm such a relationship between MT receptive field properties that we describe and motion perception.

Acknowledgements

This study was supported by the Innovational Research Incentives Scheme (VIDI) of the Netherlands Organization for Scientific Research (NWO) and the Interuniversity Attraction Poles Programme (IUAP) of the Belgian Science Policy. We thank Andre Noest, Bert van den Berg and Wim van de Grind for their contribution to this project, and Theo Stuijvenberg and our other technicians for their technical support.

Abbreviations

BI, biphasic index; LGN, lateral geniculate nucleus; MT, middle temporal cortical area; STA, spike-triggered average; V1, primary visual cortex.

Supplementary material

The following supplementary material may be found on:

<http://www.vf.bio.uu.nl/~webmanager/lab/NE/publications/IP2/methods.html>

Movie S1. Illustration of the stimulus used to map spatio-temporal receptive fields in area MT.

<http://www.vf.bio.uu.nl/~webmanager/lab/NE/publications/IP2/results.html>

Movie S2. Receptive field movie: the temporal dynamics of a receptive field of a cell in area MT (cell 237 of Fig. 2).

References

- Adelson, E.H. & Bergen, J.R. (1985) Spatiotemporal energy models for the perception of motion. *J. Opt. Soc. Am. A*, **2**, 284–299.
- Albright, T.D. (1984) Direction and orientation selectivity of neurons in visual area MT of the macaque. *J. Neurophysiol.*, **52**, 1106–1130.
- Allman, J., Miezin, F. & McGuinness, E. (1985) Direction- and velocity-specific responses from beyond the classical receptive field in the middle temporal visual area (MT). *Perception*, **14**, 105–126.
- Bair, W. & Movshon, J.A. (2004) Adaptive temporal integration of motion in direction-selective neurons in macaque visual cortex. *J. Neurosci.*, **24**, 9305–9323.
- Betts, L.R., Taylor, C.P., Sekuler, A.B. & Bennett, P.J. (2005) Aging reduces center-surround antagonism in visual motion processing. *Neuron*, **45**, 361–366.
- de Boer, R. & Kuyper, P. (1968) Triggered correlation. *IEEE Trans. Biomed. Engng.*, **15**, 169–179.
- Borghuis, B.G., Perge, J.A., Vajda, I., van Wezel, R.J., van de Grind, W.A. & Lankheet, M.J. (2003) The motion reverse correlation (MRC) method: a

- linear systems approach in the motion domain. *J. Neurosci. Meth.*, **123**, 153–166.
- Born, R.T. (2000) Center-surround interactions in the middle temporal visual area of the owl monkey. *J. Neurophysiol.*, **84**, 2658–2669.
- Born, R.T. & Tootell, R.B. (1992) Segregation of global and local motion processing in primate middle temporal visual area. *Nature*, **357**, 497–499.
- Britten, K.H. & Newsome, W.T. (1998) Tuning bandwidths for near-threshold stimuli in area MT. *J. Neurophysiol.*, **80**, 762–770.
- Britten, K.H., Shadlen, M.N., Newsome, W.T. & Movshon, J.A. (1992) The analysis of visual motion: a comparison of neuronal and psychophysical performance. *J. Neurosci.*, **12**, 4745–4765.
- Cai, D., DeAngelis, G.C. & Freeman, R.D. (1997) Spatiotemporal receptive field organization in the lateral geniculate nucleus of cats and kittens. *J. Neurophysiol.*, **78**, 1045–1061.
- Cook, E.P. & Maunsell, J.H. (2004) Attentional modulation of motion integration of individual neurons in the middle temporal visual area. *J. Neurosci.*, **24**, 7964–7977.
- Dawis, S., Shapley, R., Kaplan, E. & Tranchina, D. (1984) The receptive field organization of X-cells in the cat: spatiotemporal coupling and asymmetry. *Vis. Res.*, **24**, 549–564.
- De Valois, R.L., Cottaris, N.P., Mahon, L.E., Elfar, S.D. & Wilson, J.A. (2000) Spatial and temporal receptive fields of geniculate and cortical cells and directional selectivity. *Vis. Res.*, **40**, 3685–3702.
- DeAngelis, G.C., Ohzawa, I. & Freeman, R.D. (1995) Receptive-field dynamics in the central visual pathways. *Trends Neurosci.*, **18**, 451–458.
- Dragoi, V., Sharma, J., Miller, E.K. & Sur, M. (2002) Dynamics of neuronal sensitivity in visual cortex and local feature discrimination. *Nat. Neurosci.*, **5**, 883–891.
- Dubner, R. & Zeki, S.M. (1971) Response properties and receptive fields of cells in an anatomically defined region of the superior temporal sulcus in the monkey. *Brain Res.*, **35**, 528–532.
- Emerson, R.C., Bergen, J.R. & Adelson, E.H. (1992) Directionally selective complex cells and the computation of motion energy in cat visual cortex. *Vis. Res.*, **32**, 203–218.
- Grunewald, A. & Lankheet, M.J. (1996) Orthogonal motion after-effect illusion predicted by a model of cortical motion processing. *Nature*, **384**, 358–360.
- Hartline, H.K., Wagner, H.G. & Ratliff, F. (1956) Inhibition in the eye of *Limulus*. *J. Gen. Physiol.*, **39**, 651–673.
- Julesz, B. (1971) *Foundations of Cyclopean Perception*. University of Chicago Press, Chicago.
- Livingstone, M.S., Pack, C.C. & Born, R.T. (2001) Two-dimensional substructure of MT receptive fields. *Neuron*, **30**, 781–793.
- Macknik, S.L. & Livingstone, M.S. (1998) Neuronal correlates of visibility and invisibility in the primate visual system. *Nat. Neurosci.*, **1**, 144–149.
- Malpeli, J.G. (1998) Measuring eye position with the double magnetic induction method. *J. Neurosci. Meth.*, **86**, 55–61.
- Maunsell, J.H. & Van Essen, D.C. (1983) Functional properties of neurons in middle temporal visual area of the macaque monkey. I. Selectivity for stimulus direction, speed, and orientation. *J. Neurophysiol.*, **49**, 1127–1147.
- Mazer, J.A., Vinje, W.E., McDermott, J., Schiller, P.H. & Gallant, J.L. (2002) Spatial frequency and orientation tuning dynamics in area V1. *Proc. Natl Acad. Sci. USA*, **99**, 1645–1650.
- Mikami, A., Newsome, W.T. & Wurtz, R.H. (1986) Motion selectivity in macaque visual cortex. I. Mechanisms of direction and speed selectivity in extrastriate area MT. *J. Neurophysiol.*, **55**, 1308–1327.
- Movshon, J.A., Adelson, E.H., Gizzi, M.S. & Newsome, W.T. (1985) The analysis of moving visual patterns. In Chagas, C., Gattass, R. & Gross, C. (Eds), *Study Group on Pattern Recognition Mechanisms*. Pontificia Academia Scientiarum, Vatican City, pp. 117–151.
- Movshon, J.A., Albright, T.D., Stoner, G.R., Majaj, N.J. & Smith, M.A. (2003) Cortical responses to visual motion in alert and anesthetized monkeys. *Nat. Neurosci.*, **6**, 3; author reply 3–4.
- Murakami, I. & Shimojo, S. (1993) Motion capture changes to induced motion at higher luminance contrasts, smaller eccentricities, and larger inducer sizes. *Vis. Res.*, **33**, 2091–2107.
- Murakami, I. & Shimojo, S. (1995) Modulation of motion aftereffect by surround motion and its dependence on stimulus size and eccentricity. *Vis. Res.*, **35**, 1835–1844.
- Murakami, I. & Shimojo, S. (1996) Assimilation-type and contrast-type bias of the motion induced by the surround in a random-dot display: evidence for center-surround antagonism. *Vis. Res.*, **36**, 3629–3639.
- Pack, C.C., Berezovskii, V.K. & Born, R.T. (2001) Dynamic properties of neurons in cortical area MT in alert and anesthetized macaque monkeys. *Nature*, **414**, 905–908.
- Perge, J.A., Borghuis, B.G., Bours, R.J., Lankheet, M.J. & van Wezel, R.J. (2005) Temporal dynamics of direction tuning in motion-sensitive macaque area MT. *J. Neurophysiol.*, **93**, 2104–2116.
- Priebe, N.J., Churchland, M.M. & Lisberger, S.G. (2002) Constraints on the source of short-term motion adaptation in macaque area MT. I. The role of input and intrinsic mechanisms. *J. Neurophysiol.*, **88**, 354–369.
- Raiguel, S., Van Hulle, M.M., Xiao, D.K., Marcar, V.L. & Orban, G.A. (1995) Shape and spatial distribution of receptive fields and antagonistic motion surrounds in the middle temporal area (V5) of the macaque. *Eur. J. Neurosci.*, **7**, 2064.
- Reid, R.C., Soodak, R.E. & Shapley, R.M. (1991) Directional selectivity and spatiotemporal structure of receptive fields of simple cells in cat striate cortex. *J. Neurophysiol.*, **66**, 505–529.
- Reid, R.C., Victor, J.D. & Shapley, R.M. (1997) The use of m-sequences in the analysis of visual neurons: linear receptive field properties. *Vis. Neurosci.*, **14**, 1015–1027.
- Reulen, J.P. & Bakker, L. (1982) The measurement of eye movement using double magnetic induction. *IEEE Trans. Biomed. Engng*, **29**, 740–744.
- Ringach, D.L., Hawken, M.J. & Shapley, R. (2003) Dynamics of orientation tuning in macaque V1: the role of global and tuned suppression. *J. Neurophysiol.*, **90**, 342–352.
- Ringach, D.L., Sapiro, G. & Shapley, R. (1997) A subspace reverse-correlation technique for the study of visual neurons. *Vis. Res.*, **37**, 2455–2464.
- Rodman, H.R. & Albright, T.D. (1989) Single-unit analysis of pattern-motion selective properties in the middle temporal visual area (MT). *Exp. Brain Res.*, **75**, 53–64.
- Rowe, M.H. & Palmer, L.A. (1995) Spatio-temporal receptive-field structure of phasic W cells in the cat retina. *Vis. Neurosci.*, **12**, 117–139.
- Smith, M.A., Majaj, N.J. & Movshon, J.A. (2005) Dynamics of motion signaling by neurons in macaque area MT. *Nat. Neurosci.*, **8**, 220–228.
- Tadin, D., Lappin, J.S., Gilroy, L.A. & Blake, R. (2003) Perceptual consequences of centre-surround antagonism in visual motion processing. *Nature*, **424**, 312–315.
- Tanaka, K., Hikosaka, H., Saito, H., Yukie, Y., Fukada, Y. & Iwai, E. (1986) Analysis of local and wide-field movements in the superior temporal visual areas of the macaque monkey. *J. Neurosci.*, **6**, 134–144.
- Thiele, A., Distler, C., Korbacher, H. & Hoffmann, K.P. (2004) Contribution of inhibitory mechanisms to direction selectivity and response normalization in macaque middle temporal area. *Proc. Natl Acad. Sci. USA*, **101**, 9810–9815.
- Xiao, D.K., Raiguel, S., Marcar, V., Koenderink, J. & Orban, G.A. (1995) Spatial heterogeneity of inhibitory surrounds in the middle temporal visual area. *Proc. Natl Acad. Sci. USA*, **92**, 11303–11306.